Mechanism of Proton Transfer in Short Protonated Oligopeptides. 1. *N*-Methylacetamide and N^2-Acetyl-N^1-methylglycinamide

Petr Kulhánek,[†] Edward W. Schlag,[‡] and Jaroslav Koča*,[†]

National Centre for Biomolecular Research, Faculty of Science, Masaryk University, Kotlářská 2, CZ-611 37 Brno, Czech Republic, and Institut für Physikalische und Theoretische Chemie, Technische Universität München, Lichtenbergstrasse 4, D-85747 Garching, Germany

Received: December 11, 2002; In Final Form: April 22, 2003

A study of proton transfer in models of a single peptide unit (*N*-methylacetamide) and diamide (N^2-acetyl-N^1-methylglycinamide) as well as the influence of a single water molecule on proton transfer is presented here. Three proton pathways in protonated *N*-methylacetamide are considered: isomerization, inversion, and 1,3-proton shift. The isomerization step exhibits the lowest energy barrier. When a single water molecule was added, no significant influence on proton isomerization was observed. In the diamide model, the isomerization−jump mechanism of proton transfer along diamide carbonyl oxygens was inspected, and the proton isomerization steps were found to be the most energy-demanding processes (∼17 kcal mol^{-1}). The presence of a single water molecule leads to a different, lower-energy-barrier proton-transfer mechanism with proton exchange. The highest energy barrier is only 7.6 kcal mol^{-1}. Possible competing pathways are also discussed.

Introduction

Recently, interactions of peptides or proteins with protons have been very extensively studied both experimentally and theoretically.[1−13] There is no doubt that these interactions in a water environment play a crucial role in all biological systems. Their role starts with catalysis in many enzymatic reactions,[3] especially in amide bond hydrolysis,[4] and extends to bioenergetic proton transport.[5] From the structural point of view, the formation of hydrogen-bonded bridges between water and protonated peptides can change geometries and conformational equilibria, resulting in different biological activity. Gas-phase studies on proton transfer are becoming very important with the development of new peptide- and protein-sequencing methods based on mass spectroscopy. This is due mainly to the use of soft ionization methods such as fast atom bombardment (FAB),[14] matrix-assisted laser desorption/ionization (MALDI),[15] and electrospray ionization (ESI).[16−18] These studies are important for the understanding and interpretation of the huge amount of complex fragmentation data obtained from measured spectra.

Oligopeptides and proteins contain several positions where the proton can be attached. These are notably the terminal amino group, carbonyl oxygens, amide nitrogen atoms of peptide backbone, and also basic side chains (lysine, arginine, histidine). The best position on the peptide backbone where the proton can be bonded is the terminal amino group because it has the highest basicity.[6] The resulting ammonium salt is usually stabilized by a bridge with a terminal carbonyl oxygen.[7,8] Other sites very suitable for the attachment of a proton are carbonyl oxygens. The contact is particularly effective when the interacting proton is stabilized by another carbonyl oxygen. Two very close energy minima exist in this case with the proton between the oxygens.[10,11] These sites differ very little in electronic energies, and they are separated by only a small energy barrier. When zero-point energy is added to the final energy, the two minima disappear and the transition state between the original minima becomes a new minimum.

CHART 1

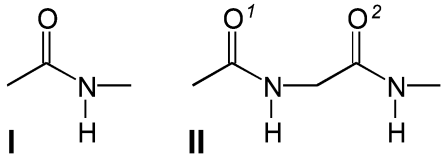

The interaction of a proton with the carbonyl oxygen of the amidic group leads to two structures, which are *E*/*Z* isomers. These two isomers can interconvert by proton isomerization around the double bond on the carbonyl group. Because this process is energy-demanding, it is probable that this step will be rate-limiting.[11] The least energy-favorable sites for proton connecting are nitrogens of amide groups. From these sites, the proton can be transferred to the neighboring carbonyl oxygen. This transfer has a very high activation barrier. However, in the presence of some protic compounds, such as water or methanol, this process proceeds via a proton-exchange mechanism with significantly smaller barriers than pure proton transfer.[13]

Here we present a study of proton transfer in *N*-methylacetamide (**I**) and N^2-acetyl-N^1-methylglycinamide (**II**) according to the peptide model (see Chart 1) with and without water molecule assistance.

The study is preferentially focused on the energy-favorable proton-transfer pathways from the first to the second terminal of the molecule. It is not the goal of this work to find all possible conformations and proton-transfer pathways between all accessible sites. Such a problem, solved by DFT study (B3LYP/6-31G*) on the similar systems, *N*-formylglycylglycinamide and

* Corresponding author. E-mail: jkoca@chemi.muni.cz.
[†] Masaryk University.
[‡] Technische Universität München.

10.1021/jp027689+ CCC: $25.00
Published on Web 07/04/2003

glycylglycine dipeptide, can be found in refs 10 and 11. However, we cannot use glycylglycine for our purposes. The main reason is that the unblocked terminal amino group either directly interacts with the proton or, at least, will have a strong influence on proton interactions with other parts of the molecule. Also, the C-terminal carboxyl group exhibits very different electronic distribution compared to the amidic group. This would influence interactions on the first and second carbonyls. Therefore, we have used different models in this paper which will, in our opinion, much better mimic the situation in a real peptide, especially that composed of a polyglycine chain. This will allow us to separate contributions coming only from the interaction with the carbonyl oxygen (model **I**) from interactions in which also the stabilizing effects of other atoms contribute (model **II**). Terminal methyl groups, which are included in both models **I** and **II**, ensure that the electron density will be almost identical to that of polyglycine. Moreover, the methyl groups also much better mimic steric interactions which may occur between the interacting proton and the model peptide. Additionally, we use the same type of functional (B3LYP) in this paper as used by the above authors,[10,11] but we include polarization functions on heavy atoms as well as hydrogens and also diffusion functions on heavy atoms. This improves mainly the description of longer-distance interactions. Generally, all the above changes imply a model situation that is closer to real peptides. This is especially important for the case when a water molecule is included. It allows us to better understand the process, and it is also on the way to transferring future studies to a biologically more realistic environment.

Computational Details

All stationary points on the potential energy surface (PES) presented here were localized at the density functional theory (DFT) level employing the hybrid B3LYP functional (using Becke's three-parameter exchange functional[19] and the correlation functional from Lee, Yang, and Parr[20,21]) with the 6-31+G** basis set in the Gaussian 98 (G98) molecular modeling package.[22] Minima were found using standard optimization technique, and first-order transition states were found using the Berny transition-state optimization algorithm with an explicitly calculated Hessian at the first optimization step. The nature of all stationary points was determined by vibrational analysis using the same method and basis set. All minima presented in this study have all real vibrational frequencies, and the first-order transition states have only one imaginary vibrational frequency.

The structures that were used for final calculations were found with the same hybrid density functional but a smaller basis set, 6-31G(d′,p′). [Two apostrophes in basis notation means parametrization by Petersson and co-workers.[23,24]] Trial structures for this calculation level were found in all cases by a proton coordinate driving. The driving was performed by relaxed potential energy surface scan implemented in G98. This technique is based on the incremental change of the proton internal coordinate with the optimization of the remaining coordinates. The distance between the proton and some oxygen atoms, or the dihedral angle defining the position around the carbonyl double bond, was usually chosen as the driven internal coordinate, with the step size from 0.1 to 0.15 Å for distance and from 10 to 15° for dihedral angle. The structure with the maximum energy was then considered to be a trial transition state and submitted to the full transition-state optimization as described above. The structures with the minimum energy were considered to be trial minimum and fully optimized.

The notation of electronic energy used in the text is the energy resulting from quantum-chemical calculation, and it is not corrected with the zero-point vibrational energy. The thermodynamic functions such as the enthalpy and Gibbs energy were calculated for 298.15 K and 101325 Pa. The zero-point vibrational energies that were used for their calculation were scaled by a standard value. Although our model contains methyl groups, the calculated thermochemistry energies are not corrected to these possible low-energy-barrier internal rotors, as we do not expect that they will make a key contribution to the final results. The relative energies are differences between energies of individual structures and a reference structure that has all energy quantities equal to zero (each model has its own reference structure).

SCHEME 1

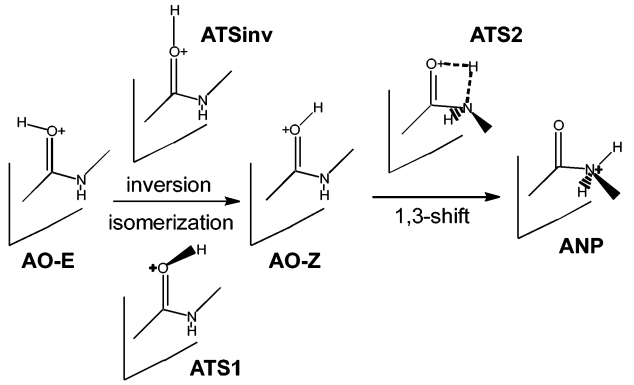

Abbreviations

The names of structures used in the paper are derived from prefixes of the studied models, e.g., **A** for *N*-methylacetamide and **DA** for N^2-acetyl-N^1-methylglycinamide, and several affixes. Affixes **O** and **N** mean an oxygen or nitrogen atom where the proton is bonded, respectively. In **DA**, we focus only on oxygen protonation; therefore, affixes **O** and **N** are not used. Affixes **Z** and **E** denote the configuration of a proton on a carbonyl double bond. If a cyclic structure is created with proton interaction, then the affix **c** is used. The presence of a single water molecule is abbreviated by the **w** affix. Carbonyl oxygens are numbered as depicted in Chart 1. All transition states are denoted by numbered **TS** affixes. Alternative structures that differ in energy are abbreviated by affix **a**.

Results and Discussion

***N*-Methylacetamide.** *N*-Methylacetamide was chosen as the simplest model which represents the situation on a single peptide unit. The proton as a strong acidic species can be bonded to basic parts of *N*-methylacetamide in three ways. Two possible positions are localized on the carbonyl oxygen, which has two lone electron pairs lying in the plane of the amide group. This situation allows the proton to be attached to oxygen in *E* (**AO-E**) or *Z* (**AO-Z**) configuration. The last place where the proton could be connected is the amide nitrogen (**ANP**), which has only one lone pair (Scheme 1).

All computational studies are dependent on the calculation methods used, and it is always necessary to validate their precision. The best way to do that is to compare their results with experimental data. Unfortunately, data that would describe proton transfer in our models are not available. However, proton affinity, which is closely related to our study and which is experimentally known for *N*-methylacetamide, can be used for the method validation. By definition, the proton affinity is the negative of the enthalpy of the hypothetical protonation reaction

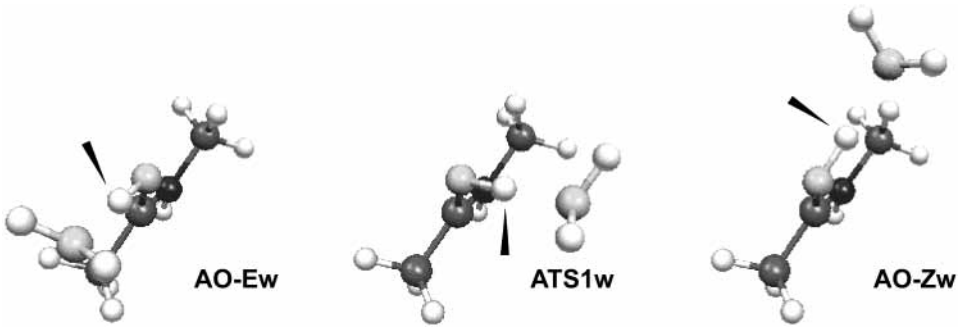

Figure 1. Water-assisted proton isomerization in protonated *N*-methylacetamide. The black arrow points at the transferred proton.

TABLE 1: Proton Transfer in Protonated *N*-Methylacetamide—Relative Electronic Energies Δ*E*, Enthalpies Δ*H*, and Gibbs Energies Δ*G* of Minima and Transition States (All in kcal mol^{-1})

structure	Δ*E*	Δ*H*	Δ*G*
AO-E	0.00	0.00	0.00
ATS1	10.75	9.42	10.53
ATSinv[a]	23.34		
AO-Z	2.75	2.58	3.20
ATS2	54.81	50.99	51.65
ANP	16.83	16.63	16.37

[a] Hypothetical transition state for the inversion process. Relative enthalpy and Gibbs energy were not calculated since the structure is optimized with constraint (for a description of the constraint, see the text).

of species M that leads to cation MH^+. The proton affinity of *N*-methylacetamide is then the negative of the enthalpy change of its protonation leading to the protonated forms, which are, however, the point of our interest.

The experimental value[25] of proton affinity for *N*-methylacetamide is 212.4 kcal mol^{-1}. The calculated proton affinities for the protonation processes that lead to all three protonated isomers, **AO-E**, **AO-Z**, and **ANP**, are 213.1, 210.5, and 196.5 kcal mol^{-1}, respectively. The highest calculated value should be a significant part of the experimental value because structure **AO-E** is the most thermodynamically stable product of all the protonation processes. The difference between this calculated value and the experimental value of proton affinity is less than 1 kcal mol^{-1}. This confirms that the method is suitable for the study of proton transfer in protonated *N*-methylacetamide and, as we assumed, also for the study of proton transfer in protonated diamide that will be discussed later.

We have considered proton transfer among all three isomers (**AO-E**, **AO-Z**, and **ANP)** of protonated *N*-methylacetamide. There are several ways that it could be performed (Scheme 1). The first is proton rearrangement from **AO-E** to **AO-Z**, which could proceed via isomerization or an inversion mechanism. The other possible way is a 1,3-proton shift from **AO-Z** to **ANP**. The direct transfer from **AO-E** to **ANP** is probably not suitable because the proton is in a very unfavorable position. Therefore, this path was not explored further.

The isomerization mechanism is accomplished by proton rotation around the carbonyl double bond from structure **AO-E** to **AO-Z**. The transition state **ATS1** of this one-step mechanism has a relative Gibbs energy of 10.5 kcal mol^{-1} with respect to structure **AO-E**, which is more stable than isomer **AO-Z** by 3.2 kcal mol^{-1} (Table 1). Interestingly, the proton in transition state **ATS1** is not situated perpendicular to the amide plane. It is about 8° shifted toward structure **AO-Z**. This can be explained by different the electronic properties of *E* and *Z* configuration half-spaces. Steric hindrance should not contribute to this shift, since the steric hindrance between the proton and the *N*-methyl group should be higher than that between the proton and the α-methyl. Therefore, this would imply exactly the opposite behavior.

TABLE 2: Water-Assisted Proton Isomerization in Protonated *N*-Methylacetamide—Relative Electronic Energies Δ*E*, Enthalpies Δ*H*, and Gibbs Energies Δ*G* of Minima and Transition State (All in kcal mol^{-1})

structure	Δ*E*	Δ*H*	Δ*G*
AO-Ew	0.00	0.00	0.00
ATS1w	10.19	8.50	10.48
AO-Zw	3.80	3.65	4.19

During the inversion mechanism, the proton always remains in the plane of the carbonyl group, and it moves by rotation around the carbonyl oxygen. Such a configuration change on a double bond is known to be preferred in the case of the azomethin derivatives.[26] However, we were not able to find any first-order saddle point for this process. To be still able to consider the pathway, we used for comparison the energy of constrained geometry in which the angle, comprised by the carbonyl carbon, the oxygen, and the attached proton, was 180°. Vibrational analysis of the hypothetical inversion transition state **ATSinv** showed that it exhibits two imaginary vibrations. Its relative electronic energy, 23.4 kcal mol^{-1} with respect to **AO-E**, is approximately 2 times higher than the barrier of the isomerization pathway.

The process with the highest activation barrier is the 1,3-proton shift between **AO-Z** and **ANP** isomers. We found that the Gibbs activation barrier toward structure **ANP** is 49.1 kcal mol^{-1}. This value is comparable to the calculated barrier on the very similar protonated formamide system,[13] which is 52.1 kcal mol^{-1} (B3LYP/6-31++G**). The difference may be ascribed to using a different basis set and mainly to the different electronic properties of the amide group due to the methyl groups in *N*-methylacetamide.

Since we were not able to find any energy-favorable inversion pathway and the isomerization pathway found has a barrier almost 4 times lower than that of the 1,3-proton shift, we only considered the isomerization path in further calculations that also included a water molecule.

If a single water molecule is coordinated to protonated *N*-methylacetamide, the energy and geometric parameters of proton isomerization are slightly changed. In isomers **AO-Ew** and **AO-Zw**, and the transition state of proton isomerization, **ATS1w**, the water molecule is connected to the system by a very strong hydrogen bond between the proton and water oxygen atom (Figure 1). The calculated energies for these structures are given in Table 2. The bond between the attached proton and the carbonyl oxygen in all structures is elongated by about 0.05 Å compared to that in protonated *N*-methylacetamide (Table 3). This effect is most noticeable in the case of transition

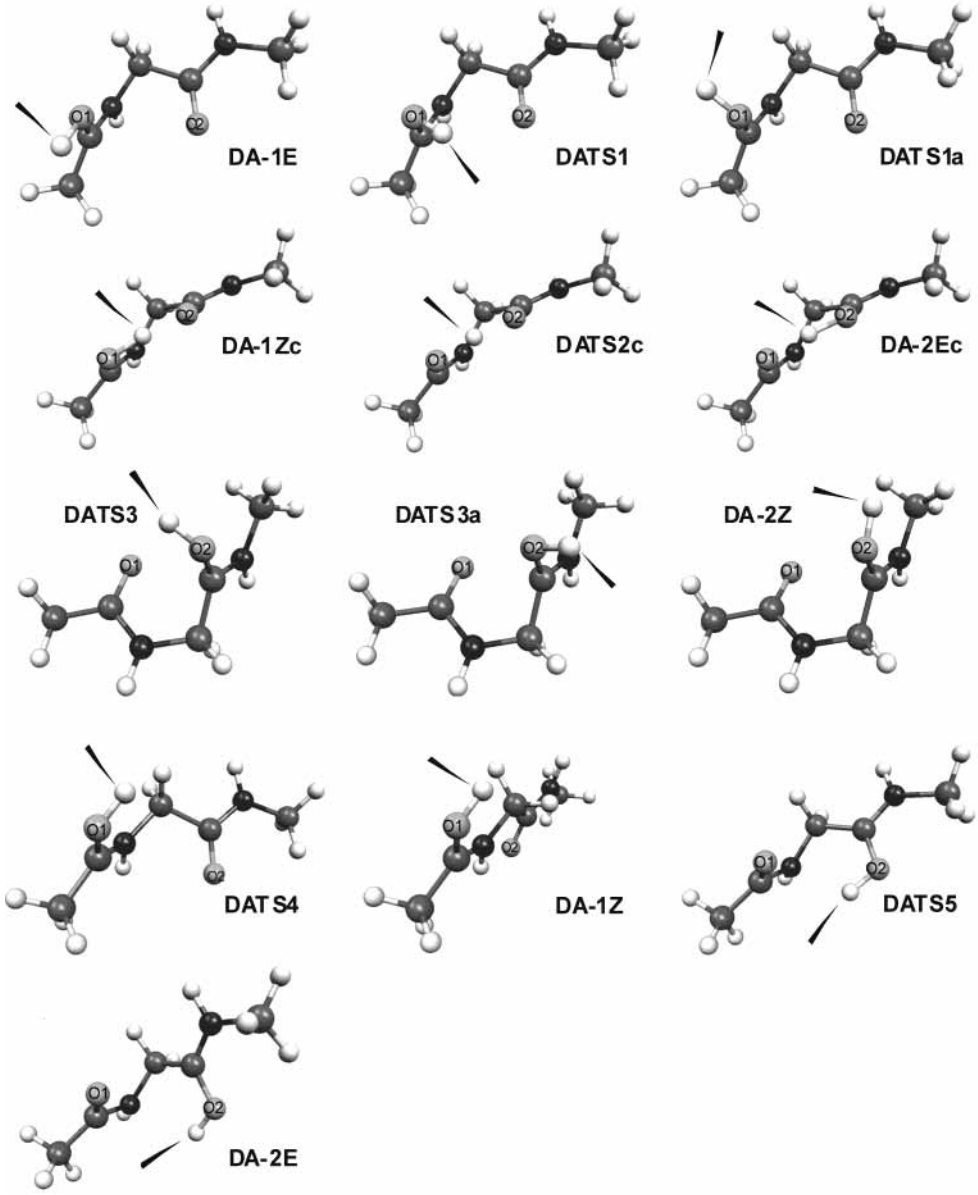

Figure 2. Stationary structures on the potential energy surface of the protonated diamide. The black arrow points at the attached proton.

TABLE 3: Comparison of Proton Isomerization in Protonated *N*-Methylacetamide without and with Single Water Molecule Stabilization (Distances *d* in Å and Dihedral Angles *D* in Degrees)

structure	D(CC=OH$^+$)	d(H$^+$—O=C)	d(C=O)	d(=C—N)	structure	D(CC=OH$^+$)	d(H$^+$—O=C)	d(C=O)	d(=C—N)	d(H$_2$O—H$^+$)
AO-E	−0.7	0.972	1.314	1.304	**AO-Ew**	0.0	1.015	1.298	1.311	1.563
ATS1	98.4	0.971	1.331	1.302	**ATS1w**	97.3	1.032	1.303	1.311	1.483
AO-Z	180.0	0.973	1.309	1.310	**AO-Zw**	179.5	1.014	1.294	1.315	1.587

state **ATS1w**, but it does not influence the isomerization energy barrier toward structure **AO-Zw**. The higher reaction Gibbs energy of proton isomerization from **AO-Ew** to **AO-Zw** might be caused by higher steric hindrance between the water and the methyl group on the amide nitrogen in structure **AO-Zw**.

Basicity of the water molecule induces the second possible proton-transfer scheme. In this hypothetical situation, the proton transfer begins by proton movement from *N*-methylacetamide to water. During the second step, the oxonium cation is moved to the opposite configuration, and the transport is finished by a backward proton jump from the oxonium cation to *N*-methylacetamide. We were not able to find a stable complex between the oxonium cation and *N*-methylacetamide while inspecting this path. The proton always jumps back to *N*-methylacetamide during optimization of such structures. The reason for this is probably the higher gas basicity of *N*-methylacetamide (204.9 kcal mol^{-1}, ref 25) than that of water (157.7 kcal mol^{-1}, ref 25). Stable complexes with an oxonium cation can be expected in the presence of more water molecules,[27] because the basicity of such a water cluster is higher.

***N*^{2}-Acetyl-*N*^{1}-methylglycinamide.** *N*^{2}-Acetyl-*N*^{1}-methylglycinamide (diamide) was used according to the peptide model for studying interactions with a proton. The natural dipeptide contains a basic amino group on the N-terminal that preferentially interacts with the proton because of its strong basicity. Therefore, we modified this dipeptide by terminal blocking (see Chart 1, **II**). This modification keeps the situation on both amidic groups similar to real oligopeptides, and the diamide used can be considered as a part of a repeating motif in glycin polypeptide.

The situation in the protonated diamide is more complicated than that in protonated *N*-methylacetamide because of the two carbonyl oxygens. Generally, the proton can be connected to carbonyl oxygens in four ways: two *E* and two *Z* configurations for each oxygen atom. However, we have localized many more stationary states for the proton interaction. In the first structure, **DA-1E**, the proton is attached to the first oxygen, O1, of the diamide in *E* configuration (see Figure 2). The similar structure **DA-2Z** has the proton connected to the second carbonyl oxygen, O2, in *Z* configuration. In both structures, **DA-1E** and **DA-2Z**, the proton is not stabilized by the adjacent oxygen O2 and O1, respectively. This is not feasible because the short chain between the carbonyl groups does not allow the proton to get closer to the adjacent oxygen. Nevertheless, the adjacent oxygen interacts with the partially charged carbon of the protonated carbonyl, which is close enough. In the opposite proton configurations (1*Z* and 2*E*), the situation is completely different. There are two structures, **DA-1Zc** and **DA-2Ec**, in which the proton is strongly stabilized by the adjacent oxygen. In the remaining two structures, **DA-1Z** and **DA-2E**, the proton is not stabilized.

We have studied the path of proton transfer leading from **DA-1E** to **DA-2Z**, which could represent proton transfer from N-terminal to C-terminal in protonated oligopeptides. The first step of the process is proton isomerization from *E* to *Z* configuration on the first carbonyl oxygen. In contrast to protonated *N*-methylacetamide, it could be performed in two ways that are distinguished by proton stabilization with the adjacent carbonyl oxygen in the transition state. The relative Gibbs energy of isomerization transition state **DATS1a** without proton stabilization is 11.1 kcal mol^{-1} with respect to **DA-1E**, and this is comparable with the value obtained for **ATS1** in protonated *N*-methylacetamide (10.5 kcal mol^{-1}). The absolute value of the proton dihedral angle (−101.1°) in **DATS1a** is also similar to that in transition state **ATS1** (98.4°). The reason for the different sign is that the isomerization takes place in the opposite half-space of the carbonyl group. In the second situation (**DATS1**), the Gibbs energy barrier with respect to **DA-1E** is 6.0 kcal mol^{-1}, which is approximately 50% lower, and the absolute value of the proton dihedral angle is smaller by about 20° with respect to that of transition state **DATS1a**. It implies that the stabilization of the proton with the adjacent carbonyl oxygen in transition state **DATS1** is very significant.

After the first isomerization step, the proton is moved to its best energy location, where both adjacent carbonyl oxygens stabilize it. There are two minima, **DA-1Zc** and **DA-2Ec**, which are separated by low-lying transition state **DATS2c**. When complete thermochemistry is taken into account, the situation is changed to one single minimum on the Gibbs energy surface that corresponds to the structure **DATS2c**. Such findings are in agreement with the conclusions in refs 10 and 11. This would imply that electron density changes on the amidic groups caused by the substitution do not principally influence the behavior of the proton when both carbonyl oxygens stabilize it. However, it is necessary to keep in mind that the geometry and electronic energy differences are very low for all three structures, **DA-1Zc**, **DATS2c**, and **DA-2Ec**. This may imply a significant inaccuracy in calculated thermodynamics contributions. Also, anharmonicity, which is another factor that may play a role, is not included in calculations because of its computational demands. Anharmonicity may be especially important in the case of **DA-1Zc** and **DA-2Ec**. Once the distance between the proton and the closer oxygen decreases, the energy of the whole structure strongly increases due to repulsion of both atoms, while the proton movement in the opposite direction does not lead to such a remarkable energy increase because the system reaches structure **DATS2c**.

TABLE 4: Relative Electronic Energies ΔE, Enthalpies ΔH, and Gibbs Energies ΔG of Minima and Transition States on the Potential Energy Surface of Protonated Diamide (All in kcal mol^{-1}), and Dihedral Angles D_1 and D_2 Describing the Relative Position of the Transferred Proton (All in deg)

structure	ΔE	ΔH	ΔG	D_1(CC═O^{1}H)[a]	D_2(CC═O^{2}H)[a]
DA-1E	0.00	0.00	0.00	4.0	
DATS1	5.76	4.50	5.98	82.1	
DATS1a	12.20	10.78	11.09	−101.1	
DA-1Zc	−9.61	−11.23	−9.97	162.1	7.9
DATS2c	−9.57	−12.48	−10.71	159.9	7.0
DA-2Ec	−9.61	−11.17	−9.90	157.1	5.9
DATS3	5.50	4.16	6.07		−108.2
DATS3a	10.85	9.42	10.75		86.0
DA-2Z	2.19	1.89	3.06		−175.2
DATS4	4.87	3.98	5.03	176.9	
DA-1Z	−0.63	−1.09	−0.85	180.0	
DATS5	0.84	−0.01	1.19		−6.0
DA-2E	−1.41	−1.47	−0.93		−9.3

[a] For oxygen atoms numbering, see Chart 1.

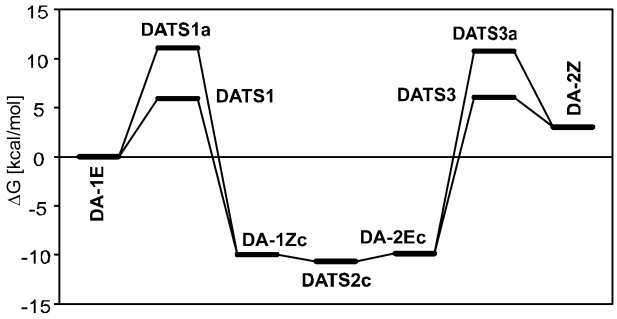

Figure 3. Gibbs energy profile of proton transfer in the protonated diamide.

The proton is located almost in the middle between the adjacent carbonyl oxygens (the distance from the first carbonyl is 1.21 Å, and that from the second one is 1.20 Å) in the most energy stable structure **DATS2c**. These distances are between the distance found for an ordinary C═O$^+$—H bond (0.97 Å in protonated *N*-methylacetamide) and the distance observed for a hydrogen bond in a complex between protonated *N*-methylacetamide and single water molecule, which is in the range from 1.48 to 1.56 Å.

The last step of proton transfer from **DA-1E** to **DA-2Z** is further isomerization on the second carbonyl group in two possible ways, again with (**DATS3**) and without (**DATS3a**) proton stabilization by the adjacent carbonyl oxygen. The calculated relative energies of all the structures are summarized in Table 4. The relative Gibbs energies described for the proton transfer discussed above are pictured in Figure 3.

Side pathways can further complicate proton transfer along the diamide chain. In the proton-transfer scheme discussed above, the proton stabilization by adjacent carbonyl oxygens in **DA-1Zc** and **DA-2Ec** structures is broken by proton isomerization on the first and second carbonyl double bonds, respectively. However, the proton can remain in its configuration, and the stabilization can also be broken by rotation of carbonyl groups with respect to each other. During breaking of the hydrogen bond between the proton and the second carbonyl oxygen in structure **DA-1Zc**, the system is passing transition structure **DATS4**, in which the oxygen of the second carbonyl still interacts with the proton but another interaction also arises with the first amide hydrogen. This interaction becomes dominant in structure **DA-1Z**. Stabilization (as in structure **DA-1E**)

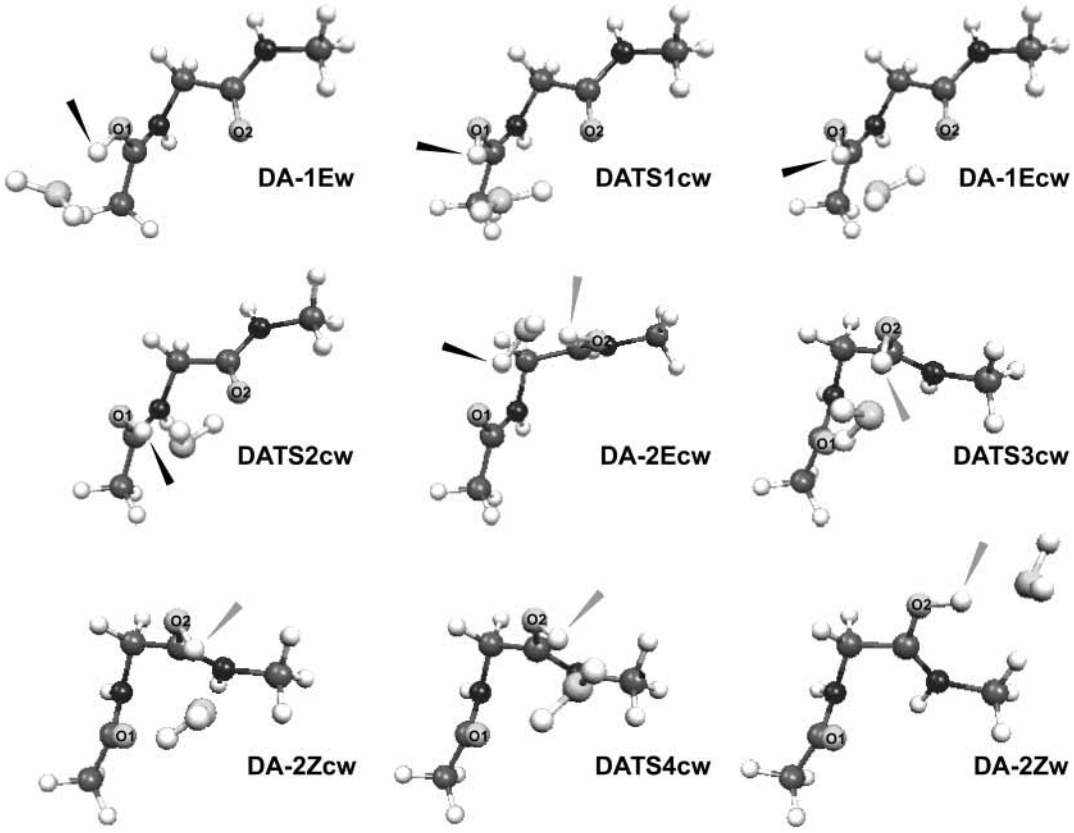

Figure 4. Water-assisted proton transfer in the protonated diamide (mechanism A). The black arrow points at the original transferred proton, and the gray one points at the proton that is transferred after proton exchange with the water molecule.

between the first carbonyl carbon and the second carbonyl oxygen is not possible due to structural restrictions (all backbone atoms are lying in one plane). On the other hand, if the bond between the proton and the first carbonyl oxygen in **DA-2Ec** is breaking, then stabilization of the proton with the first amide nitrogen exists in both the transition state **DATS5** and the final structure **DA-2E**. This interaction causes the highest out-of-plane deformation for the nitrogen of the first amide bond in **DA-2E** structure. The Gibbs energy barriers of the paths leading from **DATS2c** (minimum on the Gibbs energy surface) to **DA-1Z** and **DA-2E** structures are 15.7 and 11.9 kcal mol^{-1}, respectively. These barriers are smaller than the Gibbs energy barriers, 16.7 and 16.8 kcal mol^{-1}, of the isomerization steps leading to structures **DA-1E** and **DD-2Z**, respectively. The two structures, **DA-1Z** and **DA-2E**, are almost on the same energy level compared to geometries in which the configuration of the proton is the opposite, e.g., **DA-1E** or **DA-2Z**. This implies that proton transfer from **DA-1E** to **DA-2Z** may not be the only preferred pathway, because the hydrogen bond breaking in **DATS2c**, which exhibits similar transition energy values, may be a competing process. In other words, once the system reaches structure **DATS2c**, it may continue in the direction of proton transfer, but it also may not do so because it can be transformed into **DA-1Z** and **DA-2E**, which are out of the proton pathway along the diamide chain.

The influence of the water molecule on proton transfer in the case of the protonated diamide is much stronger than that in protonated *N*-methylacetamide. Two considerably different mechanisms of proton transfer, A and B, were found for this system. First, mechanism A will be described. The starting structure **DA-1Ew** has a configuration like that of structure **DA-1E**, except that the water molecule is bonded with a strong hydrogen bond to the proton (Figure 4). The length of this bond

TABLE 5: Water-Assisted Proton Transfer in the Protonated Diamide (Mechanism A)—Relative Electronic Energies ΔE, Enthalpies ΔH, and Gibbs Energies ΔG of Minima and Transition States (All in kcal mol^{-1}), and Dihedral Angles D_1 and D_2 Describing the Relative Position of the Transferred Proton (All in deg)

structure	ΔE	ΔH	ΔG	D_1(CC=O^{1}H)[a]	D_2(CC=O^{2}H′)[a]
DA-1Ew	0.00	0.00	0.00	2.8	
DATS1cw	2.06	1.17	4.32	40.7	
DA-1Ecw	2.06	1.71	3.21	43.0	
DATS2cw	3.10	0.56	4.36	78.9	
DA-2Ecw	−1.94	−2.95	−0.41	146.5	−9.2
DATS3cw	5.20	3.22	7.17		102.9
DA-2Zcw	4.57	4.09	6.88		133.1
DATS4cw	4.82	3.86	7.47		142.6
DA-2Zw	3.04	2.83	3.55		178.3

[a] For oxygen atoms numbering, see Chart 1. H′ means the proton originates from the water molecule. For further discussion of proton exchange, see text.

is very close to that in **A-OEw** (1.570 Å in **DA-1E**, 1.563 Å in **A-OEw**). The first step of proton transfer is to create a cyclic structure **DA-1Ecw** (transition state **DATS1cw**) in which the proton still remains in *E* configuration (dihedral angle is 40.7°; for definition, see Table 5). The water molecule forms a bridge between the proton and the second carbonyl oxygen. Proton transfer continues by proton isomerization (transition state **DATS2cw**), during which the proton exchange occurs. The result of the previous two steps is the most stable structure **DA-2Ecw**, in which the proton is connected to the second carbonyl oxygen in *E* configuration. This proton originates from one of the water hydrogens, and the proton that started the whole process becomes one of the exchanged water hydrogens. Proton transfer is then finished in two consequent steps. The first one is proton isomerization (transition state **DATS3cw**), leading to

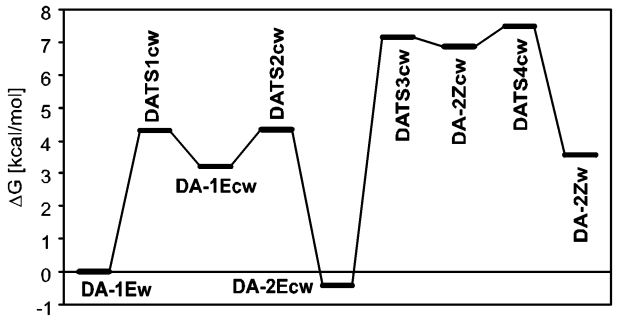

Figure 5. Gibbs energy profile of water-assisted proton transfer in the protonated diamide (mechanism A).

CHART 2

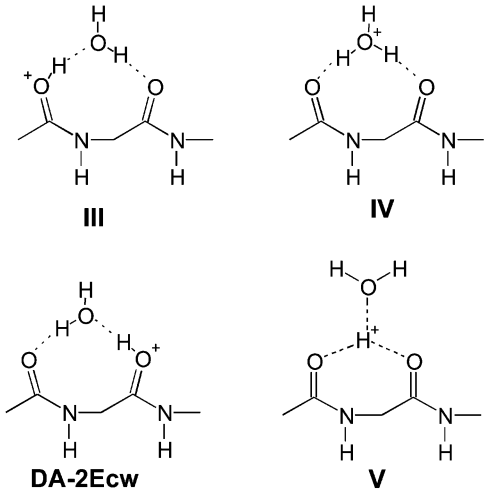

structure **DA-2Zcw**. In the last step, the water bridge is broken (transition state **DATS4cw**). In the resulting structure, **DA-2Zw**, the proton has again the same configuration as in **DA-2Z** and is stabilized by the water molecule equally as in **AO-Zw**. Calculated energies for this proton-transfer mechanism are given in Table 5.

The water-assisted proton transfer is less energy-consuming (see Figure 5). If both potential and Gibbs energy are compared with the results of proton transfer in diamide, it is apparent that the barriers in the majority of the steps are much lower. When there is no water molecule present in the calculated system, then the highest barriers on the pathways from **DA-1E** and **DA-2Z** belong to isomerization steps (Gibbs energy 6.0 and 3.0 kcal mol^{-1}, respectively). However, when a water molecule is present, then cyclic structures, **DA-1Ecw** and **DA-2Zcw**, are formed, with Gibbs barriers of 4.3 and 3.9 kcal mol^{-1}, respectively. The isomerization itself takes place with significantly smaller barriers toward the most stable structure **DA-2Ecw** (the Gibbs energy barriers are 1.2 and 0.3 kcal mol^{-1}, respectively). The water molecule also causes a decrease in the energy difference between structures **DA-1Ew** and **DA-2Zw** and the most stable structure, **DA-2Ecw**. As a consequence, the two highest energy barriers for the water-assisted proton transfer are 4.8 and 7.6 kcal mol^{-1}, respectively, compared to 16.7 and 16.8 kcal mol^{-1} for the non-water-assisted mechanism.

The lowest energy during the whole proton-transfer pathway is observed for structure **DA-2Ecw**, in which the proton is located between the two carbonyl oxygens. However, the question is whether other structures with significant stabilization effect exist in this area (Chart 2). One may imagine a situation (**III**) in which the proton is connected to the first carbonyl oxygen instead of the second one, as it is in structure **DA-2Ecw**.

TABLE 6: Water-Assisted Proton Transfer in the Protonated Diamide (Mechanism B)—Relative Electronic Energies Δ*E*, Enthalpies Δ*H*, and Gibbs Energies Δ*G* of Minima and Transition States (all in kcal mol^{-1}), and Dihedral Angles D_1 and D_2 Describing the Relative Position of the Transferred Proton (All in deg)

structure	Δ*E*	Δ*H*	Δ*G*	D_1(CC=O^{1}H)[a]	D_2(CC=O^{2}H)[a]
DA-1Ew	0.00	0.00	0.00	2.8	
DATS5w	12.05	9.67	12.17	−97.3	
DA-2Ecw	−1.94	−2.95	−0.41	146.5	−9.2
DATS6cw	−1.43	−2.45	1.09	−147.7	15.7
DA-2Ecwa	−1.44	−1.77	0.03	−138.6	20.1
DATS7w	10.27	8.49	10.28		−96.8
DA-2Zw	3.04	2.83	3.55		178.3

[a] For oxygen atoms numbering, see Chart 1.

The second possibility is the situation (**IV**) with an oxonium cation coordinated to the diamide. The last possibility (**V**) leads to the water molecule being coordinated to the proton that is located between adjacent carbonyl oxygens. Unfortunately, we did not succeed with any attempts to find any of these hypothetical structures. Structure **IV** is probably not stable because of the low basicity of the water molecule. Here, the situation is very similar to those discussed in the case of the second hypothetical proton-transfer mechanism in *N*-methylacetamide. Structure **V** probably does not exist because of greater stress in the smaller cycle. It is apparent that the number of freely rotatable bonds is higher for **DA-2Ecw** (four torsions) than for **V** (only two torsions). Structure **III** is very similar to structure **DA-2Ecw**. Therefore, we expected to find it but failed in this attempt. One of the reasons could be the different basicity of the two carbonyl oxygen sites, 1*Z* and 2*E*.

Proton transfer in the protonated diamide with a single water molecule can also proceed by a different mechanism (mechanism B). The configuration change from *E* to *Z* that occurs on both carbonyl oxygens is different for this mechanism compared to mechanism A. While two steps are necessary for such a change in mechanism A, only one step (direct isomerization) is required in mechanism B. Proton transfer will be considered to go from **DA-1Ew** to **DA-2Zw** for easier comparison of both mechanisms. The first step begins with proton isomerization on the first carbonyl double bond, leading to structure **DA-2Ecw**. The proton in the transition state of this step, **DATS5w**, is attached in the opposite half space of the amide bond (Figure 6), so the water molecule cannot form a bridge with the adjacent carbonyl oxygen as it was in mechanism A. However, the adjacent carbonyl oxygen stabilizes the whole structure by interaction of the partially charged carbonyl group carbon with the attached proton. As has been shown in mechanism A, also here proton exchange with a water molecule occurs during the first isomerization step. In the next step, a small conformation change across transition state **DATS6cw** to structure **DA-2Ecwa** occurs on the diamide chain. Proton transfer is then finished by proton isomerization (**DATS7w**) on the second carbonyl double bond, with the same geometry characteristics as in the first step. A summary of the calculated energies for mechanism B is given in Table 6, and the Gibbs energy profile of the whole pathway from **DA-1Ew** to **DA-2Zw** structure is shown in Figure 7. It is apparent from comparison of the two mechanisms that the rate-determining step in mechanism B has a higher Gibbs energy barrier (12.5 kcal mol^{-1}) than that in mechanism A (7.6 kcal mol^{-1}). This confirms that the water stabilization via bridges found in mechanism A is necessary for low-energy-barrier proton transfer.

It was found in the study of proton transfer in diamide that some pathways from structure **DATS2c** compete with the direct

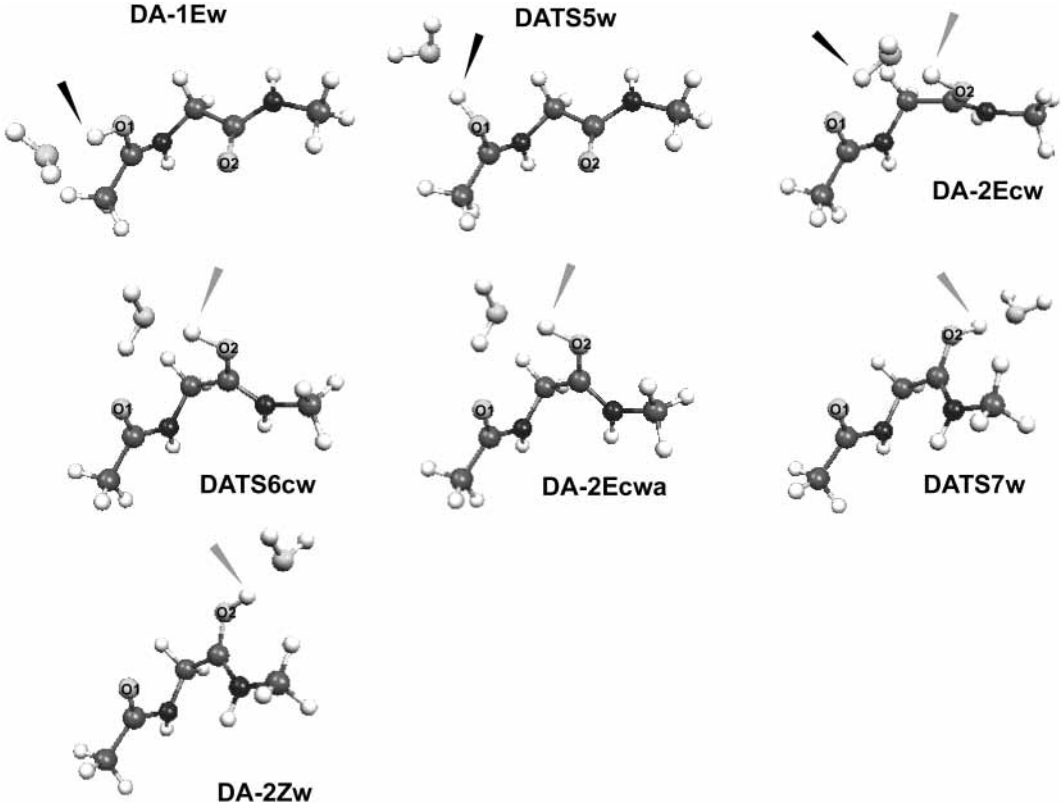

Figure 6. Water-assisted proton transfer in the protonated diamide (mechanism B). The black arrow points at the original transferred proton, and the gray one points at the proton that is transferred after proton exchange with the water molecule.

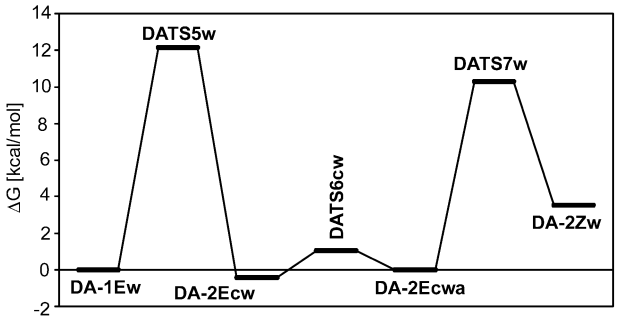

Figure 7. Gibbs energy profile of water-assisted proton transfer in the protonated diamide (mechanism B).

proton transfer along the diamide chain. Some competing pathways will be presented here. The structure of our interest is now **DA-2Ecw**. It has geometry similar to that of structure **DATS2c** but is more flexible due to the presence of the water molecule. Two side pathways were found. In the first pathway, the bond between the proton and the second carbonyl oxygen in the starting structure **DA-2Ecw** is longer. Since this is a regular bond (not a hydrogen bond), proton exchange with one of the water hydrogen atoms occurs. It must be noted that the exchange is already finished when the system reaches transition state **DATS8w** (Figure 8). The resulting structure of this process is **DA-1Zw**. In this structure, the proton is situated in configuration *Z* on the first carbonyl oxygen, and the second carbonyl oxygen interacts with the hydrogen of the first amide group. Structure **DA-1Zw** is less stable than the starting structure **DA-2Ecw** by about 1 kcal mol^{-1}, and the process has the Gibbs energy barrier about 6 kcal mol^{-1} toward the resulting structure. In the second possible pathway, the hydrogen bond between the first carbonyl oxygen and the water hydrogen atom is broken. Unfortunately, the transition state of this process was not fully localized, and only a guess structure from proton driving is

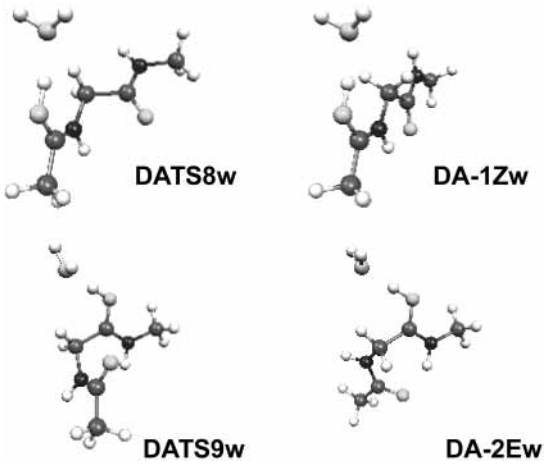

Figure 8. Important structures on two pathways competing with water-assisted proton transfer along the diamide chain.

presented as transition state **DATS9w**. The resulting structure of this pathway is structure **DA-2Ew**, in which the proton is situated in *E* configuration on the second carbonyl oxygen and the structure is stabilized by the interaction of the first carbonyl oxygen with the hydrogen atom of the second amide group, similar to the observation in structure **DA-1Zw**. The electronic energy barrier of this process (1.93 kcal mol^{-1}) is smaller than that for the first pathway because a weaker hydrogen bond is breaking. The calculated relative energies along the both pathways are collected in Table 7.

Conclusions

We have shown that the most favorable path of proton transfer in *N*-methylacetamide is the isomerization process with Gibbs energy barrier 10.5 kcal mol^{-1} (from *E* proton configuration).

TABLE 7: Relative Electronic Energies ΔE, Enthalpies ΔH, and Gibbs Energies ΔG of Structures of Two Pathways Competing the Water-Assisted Proton Transfer along the Diamide Chain (All in kcal mol^{-1})

structure	ΔE	ΔH	ΔG
DA-1Ecw	0.00	0.00	0.00
DATS8w	6.81	7.18	6.32
DA-1Zw	2.37	3.09	0.86
DATS9w[a]	1.93		
DA-2Ew	−0.18	0.85	−0.35

[a] Not all convergence criteria were fulfilled during transition-state optimization. Therefore, thermodynamic properties are not shown.

Other processes such as proton inversion or 1,3-proton shift to a nitrogen atom have significantly higher barriers. When a single water molecule is present, then the distances between the attached proton and the carbonyl oxygens are longer. The largest geometry change is exhibited in the transition state. The influence on the Gibbs energy barrier is negligible.

We have also shown that the calculated proton affinities of *N*-methylacetamide are in very good agreement with experimental data. On the basis of this observation, we assume that all the minima proposed by the calculations are relevant. However, we may not be so thoroughly convinced about transition states. In that case, it would be necessary to compare more experimental data.

In the case of N^2-acetyl-N^1-methylglycinamide, the most energy-favorable state is a structure in which the proton is connected between adjacent carbonyl oxygens. There are two minima localized on the PES with almost the same energy and separated by a transition state with a very low barrier. When full thermodynamics is included, this transition state becomes the most favorable structure. The proton is then placed approximately in the middle between two carbonyl oxygens, and it may be transferred into outside positions by an isomerization mechanism. These isomerization processes are usually accompanied by high energy barriers (up to 16.8 kcal mol^{-1}, and even up to 22.6 kcal mol^{-1} if the proton is not stabilized in the transition states of isomerization). Water-assisted proton transfer exhibits more significant variation than there is in the case of *N*-methylacetamide. Two considerable different mechanisms were found. In both of them, the energy differences between energy minima are smaller due to water stabilization. The two mechanisms mainly differ in their isomerization steps. In the first mechanism, water bridges stabilizing the transferred proton are formed, which results in a rate-determining Gibbs energy barrier of 7.6 kcal mol^{-1}. This stabilization is not possible in the second mechanism, which leads to a higher rate-determining Gibbs energy barrier of 12.6 kcal mol^{-1}. It was also found that a proton exchange with the water molecule occurs in both mechanisms.

Some pathways that compete with proton transfer were found in both diamide and diamide with a single water molecule. The energy barriers of these competing processes are even smaller than the barriers of the corresponding steps on the pathway of proton transfer along the diamide chain. Since the energy differences between the minima and transition states are not very dramatic in the two models, we assume that all proton-transfer processes and also competing processes are reversible.

In conclusion, water-assisted proton transfer substantially decreases energy barriers. It may be even more remarkable for longer peptide chains, which are the subject of our further studies.

Acknowledgment. We thank the Supercomputing Center in Brno, Czech Republic, for providing us with computational resources. This work has been supported by the Ministry of Education of the Czech Republic (Grant LN00A016). The authors are grateful to Mr. Roger Turland for language corrections. We are also grateful to anonymous reviewers who have contributed constructive critical comments.

Supporting Information Available: Tables containing absolute energies, enthalpies, and Gibbs energies (in a.u.) for all structures, imaginary frequencies (in cm^{-1}) for all transition structures, and Cartesian coordinates (in Å) of all structures. This material is available free of charge via the Internet at http://pubs.acs.org.

References and Notes

(1) Green, M. K.; Lebrilla, C. B. *Mass Spectrom. Rev.* **1997**, *16*, 53.
(2) Martin, R. B. *Met. Ions Biol. Syst.* **2001**, *38*, 1.
(3) (a) Richard, J. P.; Amyes, T. L. *Curr. Opin. Chem. Biol.* **2001**, *5*, 626. (b) Hur, O.; Niks, D.; Casino, P.; Dunn, M. F. *Biochemistry* **2002**, *41*, 9991.
(4) Pelmenschikov, V.; Blomberg, M. R. A.; Siegbahn, P. E. *J. Biol. Inorg. Chem.* **2002**, *7*, 284.
(5) (a) Tomashek, J. J.; Brusilow, W. S. A. *J. Bioenerg. Biomembr.* **2000**, *32*, 493. (b) Senior, A. E. *Annu. Rev. Biophys. Biophys. Chem.* **1990**, *19*, 7.
(6) Cassady, C. J.; Carr, S. R.; Zhang, K.; Chung-Phillips, A. *J. Org. Chem.* **1995**, *60*, 1704.
(7) Campbell, S.; Rodgers, M. T.; Marzluff, E. M.; Beauchamp, J. L. *J. Am. Chem. Soc.* **1995**, *117*, 12840.
(8) Wu, J.; Gard, E.; Bregar, J.; Green, M. K.; Lebrilla, C. B. *J. Am. Chem. Soc.* **1995**, *117*, 9900.
(9) Paizs, B.; Lendvay, G.; Vékey, K.; Suhai, S. *Rapid Commun. Mass Spectrom.* **1999**, *13*, 525.
(10) Csonka, I. P.; Paizs, B.; Lendvay, G.; Suhai, S. *Rapid Commun. Mass Spectrom.* **2000**, *14*, 417.
(11) Paizs, B.; Csonka, I. P.; Lendvay, G.; Suhai, S. *Rapid Commun. Mass Spectrom.* **2001**, *15*, 637.
(12) Paizs, B.; Suhai, S. *Rapid Commun. Mass Spectrom.* **2001**, *15*, 2307.
(13) Rodriquez, C. F.; Cunje, A.; Shoeib, T.; Chu, I. K.; Hopkinson A. C.; Siu K. W. M. *J. Phys. Chem. A* **2000**, *104*, 5023.
(14) Barber, M.; Boddoli, R. D.; Sedgwick, R. D.; Tyler, A. N. *J. Chem. Soc., Chem. Commun.* **1981**, 325.
(15) Hillenkamp, F.; Karas, J.; Beavis, R. C.; Chait, B. T. *Anal. Chem.* **1991**, *63*, 1193.
(16) Fenn, J. B.; Mann, M.; Meng, C. K.; Womg, S. F.; Whitehouse, C. M. *Mass Spectrom. Rev.* **1990**, *9*, 37.
(17) Smith, R. D.; Loo, J. A.; Edmonds, C. G.; Barinaga, C. J., Udseth, H. R. *Anal. Chem.* **1990**, *62*, 882.
(18) Smith, R. D.; Loo, J. A.; Barinaga, C. I.; Edmonds, C. G.; Udseth, H. R. *J. Am. Soc. Mass Spectrom.* **1990**, *62*, 882.
(19) Becke, A. D. *J. Chem. Phys.* **1993**, *98*, 5648.
(20) Lee, C.; Yang, W.; Parr, R. G. *Phys. Rev. B* **1988**, *37*, 785.
(21) Miehlich, B.; Savin, A.; Stoll, H.; Preuss, H. *Chem. Phys. Lett.* **1989**, *157*, 200.
(22) Frisch, M. J.; Trucks, G. W.; Schlegel, H. B.; Scuseria, G. E.; Robb, M. A.; Cheeseman, J. R.; Zakrzewski, V. G.; Montgomery, J. A.; Stratmann, R. E., Jr.; Burant, J. C.; Dapprich, S.; Millam, J. M.; Daniels, A. D.; Kudin, K. N.; Strain, M. C.; Farkas, O.; Tomasi, J.; Barone, V.; Cossi, M.; Cammi, R.; Mennucci, B.; Pomelli, C.; Adamo, C.; Clifford, S.; Ochterski, J.; Petersson, G. A.; Ayala, P. Y.; Cui, Q.; Morokuma, K.; Malick, D. K.; Rabuck, A. D.; Raghavachari, K.; Foresman, J. B.; Cioslowski, J.; Ortiz, J. V.; Baboul, A. G.; Stefanov, B. B.; Liu, G.; Liashenko, A.; Piskorz, P.; Komaromi, I.; Gomperts, R.; Martin, R. L.; Fox, D. J.; Keith, T.; Al-Laham, C. Y.; Peng, A.; Nanayakkara, M.; Challacombe, P. M. W.; Gill, B.; Johnson, W.; Chen, M. A.; Wong, M. W.; Andres, J. L.; Gonzalez, C.; Head-Gordon, M.; Replogle, E. S.; Pople, J. A. *Gaussian 98*, Revision A.9; Gaussian, Inc.: Pittsburgh, PA, 1998.
(23) Petersson, G. A.; Al-Laham, M. A. *J. Chem. Phys.* **1991**, *94*, 6081.
(24) Petersson, G. A.; Bennett, A.; Tensfeldt, T. G.; Al-Laham, M. A.; Shirley, W. A.; Mantzaris, J. *J. Chem. Phys.* **1988**, *89*, 2193.
(25) (a) Hunter, E. P.; Lias, S. G. *NIST Chemistry WebBook*, http://webbook.nist.gov/chemistry. (b) Hunter, E. P.; Lias, S. G. *J. Phys. Chem. Ref. Data* **1998**, *27*, 3, 413.
(26) Hofmann, H. J.; Cimiraglia, R.; Tomasi, J. *Theochem* **1987**, *37*, 19.
(27) Chaudhuri, C.; Jiang, J. C.; Wu, C.-C.; Wang, X.; Chang, H.-C. *J. Phys. Chem. A* **2001**, *105*, 8906.